applied optics

Wink-controlled polarization-switched telescopic contact lenses

Glenn M. Schuster,[1,*] Ashkan Arianpour,[1] Scott Cookson,[2] Arthur Zhang,[2] Lee Hendrik,[3] Tyrone O'Brien,[3] Agusto Alvarez,[3] and Joseph E. Ford[1]

[1]Department of Electrical & Computer Engineering, University of California San Diego, 9500 Gilman Drive, La Jolla, California 92093, USA
[2]Innovega Inc., Bellevue Way NE, Ste. 400, Bellevue, Washington 98004, USA
[3]Rockwell Collins Optronics, 2752 Loker Ave. W, Carlsbad, California 92010, USA
*Corresponding author: gschuster@eng.ucsd.edu

Received 17 August 2015; revised 2 October 2015; accepted 14 October 2015; posted 15 October 2015 (Doc. ID 248003); published 9 November 2015

We describe a wink-controlled hands-free switching system for eye-borne telescopic vision, based on a previously tested fixed-magnification telescope embedded within scleral contact lenses. Here we integrate orthogonal polarizers into the contact lens covering the F/9.1 refractive 1× and F/9.6 catadioptric 2.8× vision paths, to allow switching via external liquid crystal shutters. We provide hands-free control by an infrared wink/blink monitor, using passive retroreflectors embedded within the contact lenses. We demonstrate system operation of the self-contained switching eyewear and the modified contact lenses with a life-size human eye model with mechanical "eyelids."

OCIS codes: (110.6770) Telescopes; (170.4460) Ophthalmic optics and devices; (220.0220) Optical design and fabrication; (220.4830) Systems design.

http://dx.doi.org/10.1364/AO.54.009597

1. INTRODUCTION

Research into systems for human vision enhancement is being stimulated by interest in high mobility on-demand magnification for military, sports, and low-vision applications. In an attempt to treat bilateral end-stage age-related macular degeneration, low-magnification refractive telescopes [1–5] and a two-mirror reflective Cassegrain telescope [6] have been successfully implanted into the posterior chamber of patients' eyes. These visual prosthetic devices do not provide active switching between enhanced and normal unmagnified vision and rely on the patient developing an adaptation strategy for volitional eye selection, a processes that can be trained through the use of polarizing test spectacles [1].

A less invasive approach is to embed the telescope into eye-mounted contact lenses. An early demonstration incorporated a 2× magnification refractive telescope [7], but the 4.4 mm thick lens was impractical even for short-term wear. This optical thickness can be dramatically reduced using a multiple concentric reflection layout [8]. The first demonstration of an afocal catadioptric Galilean telescope with the required contact lens geometry used four reflections and a diffractive optic for achromatization [9]. This led to a wearable scleral contact lens with a 2.8× magnification four-reflection telescope in a 1.6 mm center thickness, where the diffractive element was replaced by a refractive achromat using a combination of polymethyl methacrylate (PMMA) and a high-index rigid gas permeable contact lens material. This lens was fabricated and used in a small-cohort clinical test [10].

Catadioptric contact lenses offer higher magnification and light collection, and a less invasive and reversible enhancement than surgically implanted vision aids. However, a lack of switching still precludes use for on-demand magnification. To eliminate the need for hand-held binoculars for soldiers, and to provide binocular accommodation for age-related macular degeneration and other retinal illnesses, active hands-free switching needs to be integrated into these systems.

In principal, an optoelectronic system with active shutters or moving optics could be incorporated within the contact lens, but the integration of the necessary electronics, actuation, and power would represent a considerable challenge. A significantly simpler path to on-demand magnification is to use passive polarization filtering optics within the contact lens, moving the active electronics to eyewear with polarization switching. The magnification could be controlled with a temple-mounted switch, but the better solution would be to offer hands-free control. This paper describes the fabrication and test of such a hands-free switching system for use with previously reported eye-borne telescopic contact lenses [10] where detailed optical design, tolerancing, and performance characterization are described. This switching system (which may also be applicable

with surgically implanted telescopes) enables rapid and intuitive selection of normal and enhanced vision.

The system conceptualized in Fig. 1 consists of external glasses with linear polarizers in front of liquid crystal (LC) elements to rotate the transmitted light polarization. Switching is controlled by active monitoring of the user's winks and blinks via a NIR LED and detector under each eye. The controller activates the LC elements (switching to magnified vision) upon detection of a left eye wink and deactivates the LC voltage (switching to 1× vision) when a right eye wink is detected. Blinking is involuntary, but always involves both eyes. Since both eyes are monitored simultaneously, blinking is detected and ignored by the system. The LC shutters are completed by internal orthogonal circular and annular polarizers embedded over the two apertures within the contact lens along with a diffusing retroreflector to enable a strong and detectable change in reflection between an open and closed eye.

This paper is organized as follows. Section 2 describes the fabrication and characterization of the scleral contact lens telescope reported in [10], now including the orthogonal linear polarizers and retroreflector needed for switching. Section 3 details the function and component characterization of the external switching system, including the fully self-contained control electronics. Finally, Section 4 describes the functional testing using a wearable contact lens mounted on a life-sized model eye [11] to enable optical bench characterization of the overall system.

2. CONTACT LENS

The telescopic contact lens includes optics related to the two vision paths and embedded polarizers and a diffusing retroreflector as part of the active hands-free switching system. Magnified vision is achieved by a F/9.6 four-reflection afocal telescope with an 2.78 mm inner radius and 4.1 mm outer radius annular aperture utilizing a low-index ($n = 1.49$) PMMA and high-index ($n = 1.54$) Paragon HI-154 rigid gas permeable polymer. The PMMA acts as the "crown" and the HI-154 acts as the "flint" in an achromatic doublet that corrects for the color aberration introduced by refraction at the necessarily curved input surface.

The key aspect of this optical design is that the 2.8× magnification telescope provides an annular input aperture that does not interfere with the central aperture, leaving it available for an independent 1× vision path. The unmagnified F/9.1 vision path passes through a 1.99 mm diameter circular aperture. Both the 1× and 2.8× optical paths are shown in Fig. 2, where the lens is depicted as mounted on the Zemax model eye. A detailed optical design, tolerancing, performance characterization, defect analysis, as well as further discussion of scleral lens wearability can be found in [10].

The switching subsystem internal to the contact lens includes a linear polarizer over the circular 1× vision aperture, and a second orthogonal linear polarizer over the annular 2.8× vision aperture. Scleral contact lenses can correct for astigmatic user prescriptions, and are designed to remain substantially stable once seated on the sclera (white) of the eye. This means that the circular central 1× polarizer and the annular outer 2.8× linear polarizers are oriented with respect to the polarization eyewear.

To enable hands-free control, a NIR LED light source and optical detector are mounted to the eye-wear to detect winks. This relies on differentiation between the reflectivity of an open and closed eye. In order to provide a strong signal invariant to external conditions and skin tone, a retroreflector is embedded within the lens in a region not obscured by the eyelids when open nor in the 1× or 2.8× optical paths. A perfect retroreflector would direct the return signal exactly back to the source, requiring a beam splitter to deflect the return signal to a detector. Instead, we used a small-angle diffuser, which allows the return signal to be collected by a detector located behind a small area LED source, as shown in Fig. 1. Since the lens is rotationally aligned to the external LC shutter glasses, a single diffusing retroreflector, located near the bottom of the lens, proved sufficient to enable hands-free switching.

The contact lens incorporates a number of elements necessary for multiple vision paths, switching, and for scleral lens

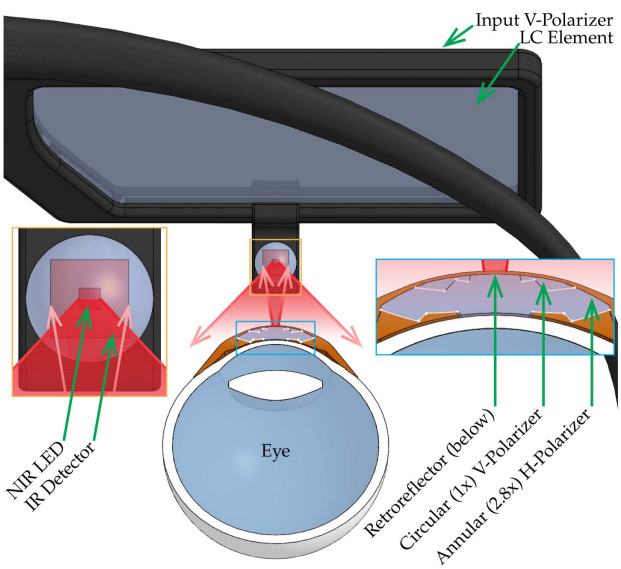

Fig. 1. Conceptual diagram of switching system showing the LC element, NIR LED and detector, contact lens with embedded retroreflector and polarizers, and eye to scale. The contact lens and eye are shown as cross sections to reveal internal structure.

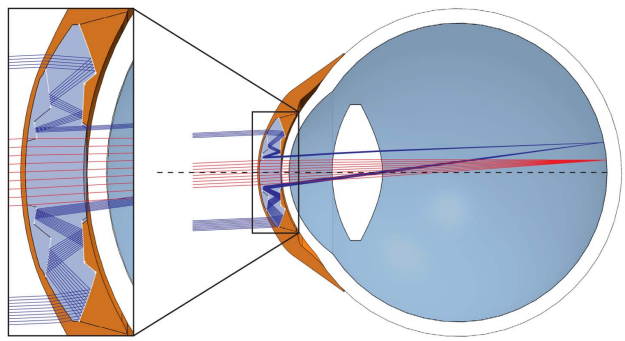

Fig. 2. Optical ray trace at a 2.5° field angle through the 1× (red) and 2.8× (blue) apertures of the contact lens when mounted to a model human eye with zoomed inset showing the folded optical path. The optical axis is shown as a dotted line.

wear. The overall structure of the scleral lens is formed of a HI-154 rigid gas permeable polymer (indicated in orange, and labeled as "top handle"). The two orthogonal polarizers lie below this layer, defining the 1× and 2.8× vision paths, along with a 0.8 mm diameter circular retroreflector for switching control. The "center insert" is a precision diamond turned element that has all of the four reflective surfaces, which are the critical alignment structures in this optical system. The two remaining elements are the top and bottom index fills, made of PMMA and HI-154, respectively. These are necessary to allow for unaberrated peripheral vision through the central 1× polarizer and around the edges of the innermost (final) annular mirror. Many of these elements are too small to be machined as discrete components and hand-assembled, so fabrication of this complex structure requires the process summarized in Fig. 3. A 3D CAD model of the contact lens is shown in Fig. 4.

A. Polarizer Preparation

The lens uses commercially available polyvinyl alcohol (PVA) linear polarizers, chosen for their minimal thickness after removing their substrate. The polarizer materials are prepared for integration by removing the thick backing of a bulk sheet of linear polarizer material leaving 18 μm of polarizing PVA. The thin sheet is then punched into a circular disk (1× aperture) and an annular ring (2.8× aperture) and are thermoformed to the proper shape, as shown in Fig. 3(b). Both the punches and molds were designed to yield the proper curvature and size after thermoforming.

B. Diffusing Retroreflector

The embedded diffusing retroreflector was made by modifying a commercially available aluminum-coated corner cube structure by stripping the substrate and adding an engineered surface-relief diffuser with a laminate coating. A negative polydimethylsiloxane (PDMS) mold of a 1 in. diameter RPC Photonics EDRG-40-9-A-1r 40° full-width half-maximum (FWHM) engineered ring diffuser was coated with trichlorosilane through vapor deposition under vacuum. The bulk of the adhesive backing of a Reflexite P66-1541 retroreflector sheet was removed with an acetone-soaked clean room wipe, followed by sonication in a 50% acetone mixture. Optical adhesive NOA 72 ($n = 1.56$) was deposited onto the top of the retroreflector sheet and the PDMS mold of the diffuser was lowered, imprinting the structure on the adhesive layer and cured. The PDMS mold was removed and a thin layer of NOA 144 ($n = 1.44$) optical adhesive was bonded to the top of the imprinted diffuser to prevent the high-index optical adhesive used in lens assembly from index-matching out the holographic structure. Finally, a 0.8 mm disk is punched from the sheet of laminated diffusing retroreflector to yield a 200 μm thick sample. A simplified representation of this process is shown in Fig. 3(a).

The angular dependence of reflected power for several combinations of retroreflector material and imprinted diffusers with and without laminate coatings was measured [Fig. 5(a)] using a 632.8 nm HeNe laser and a beam splitter to direct the reflected light into an optical power meter. In the switching system, a bare retroreflector without a diffuser [Fig. 5(b)] would direct the incident light back into the NIR LED and fail to be gathered by the collection lens and directed toward the detector. The goal of the imprinted diffuser and laminate is to maximize the reflected power between the boundary of the NIR LED and that of the collection lens. The 40° FWHM ring diffuser paired with the P66 retroreflector [Fig. 5(c)] maximized this collected power when compared to the other tested samples for a collection efficiency of 81% compared to the 44% of the bare retroreflector material.

C. Lens Assembly

The contact lens is assembled through a process shown in Fig. 3(c) which uses successive bonding and diamond turning to gradually create the complex structure and embedded elements required for the system. A precision PMMA "center insert" is diamond turned and coated with enhanced aluminum in the desired locations by ISP Optics and bonded with the flexible medical grade Dymax 141-M ($n = 1.507$) optical adhesive between a complementary (in optical regions) Paragon HI-154 polymer "bottom fill" and a PMMA "top fill" (where reservoirs allow room for excessive adhesive and air to flow). This "triple stack" is diamond turned by Paragon Vision Sciences, removing the top center nonoptical mirror (which

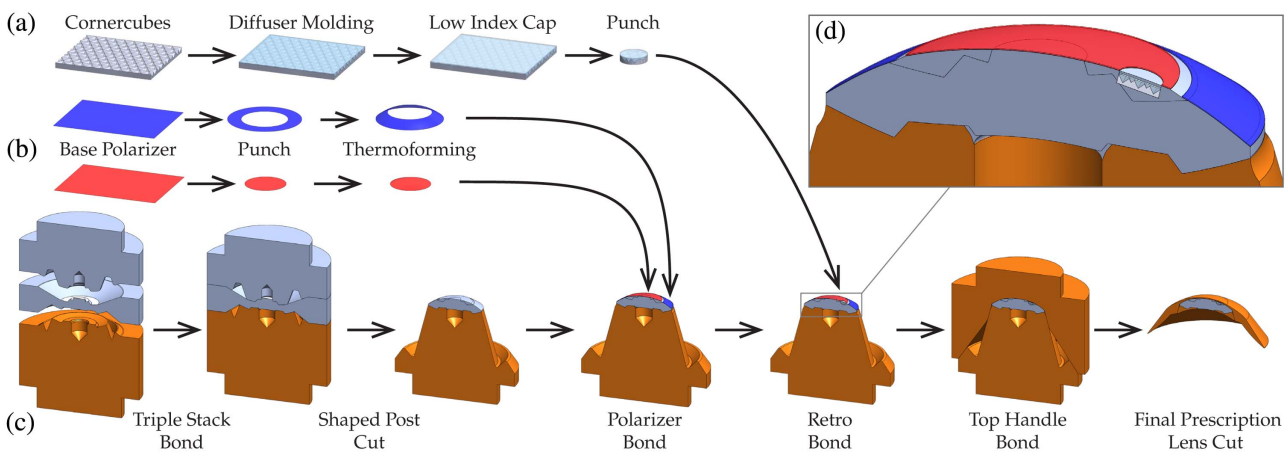

Fig. 3. CAD model illustration of the lens assembly process flow including (a) diffusing retroreflector fabrication, (b) polarizer fabrication, (c) contact lens fabrication, and (d) a zoomed inset of the polarizer and retroreflector bond.

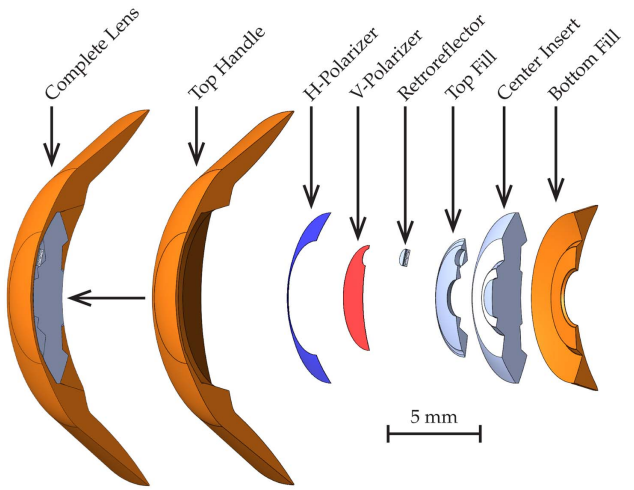

Fig. 4. CAD model of cross-sectioned assembled lens (left) and exploded view (right) showing the various elements of the design.

was 50 μm above the desired location) for precision registration to produce a "shaped post" where most of the "top fill" has been removed.

The punched and thermoformed polarizers are placed and aligned orthogonally in a negative PDMS mold of the "shaped post." The PVA polarizer and PDMS interface provides a seal which prevents adhesive from flowing over the top of the polarizers. The polarizers are attached using a more rigid medical grade UV-cure adhesive Dymax 210-CTH ($n = 1.50$). The adhesive is deposited on the concave surface of the polarizers resting on the negative PDMS mold, which is inverted and brought down on the "shaped post" and then cured (as UV light is transmitted through PDMS). The negative PDMS mold is peeled off leaving polarizers bonded to the "shaped post."

The retroreflector disk is mounted into a recess machined through the polarizer using a five-axis precision mill. An approximately 800 μm diameter and 275 μm deep recess is cut at 13.5° from normal above the second mirror at the edge of the center polarizer. This recess is aligned to the bottom of the lens with respect to the axis of the linear polarizers so the readily visible retroreflector can serve as an alignment indicator for placement on the eye. The part is cleaned of debris and the prepared diffusing retroreflector is placed in the drilled hole above a small amount of adhesive.

The "shaped post" with bonded polarizers and diffusing retroreflector shown in the enlargement inset in Fig. 3(d) is then covered by a complementary Paragon HI-154 polymer "top handle," attached with Dymax 210-CTH optical adhesive, to form the piece ready to be machined to the individual user prescription.

This final part is diamond tuned by Paragon Vision Sciences into a scleral lens, where the lower surface matches the profile and correct rotational alignment required by the user for a comfortable fit, and the upper surface includes the user-specific optical prescription on both the 1× and 2.8× aperture areas. This yields the final lens shown in Fig. 6. This specific lens has a zero diopter prescription, for use in the system testing on the laboratory model eye.

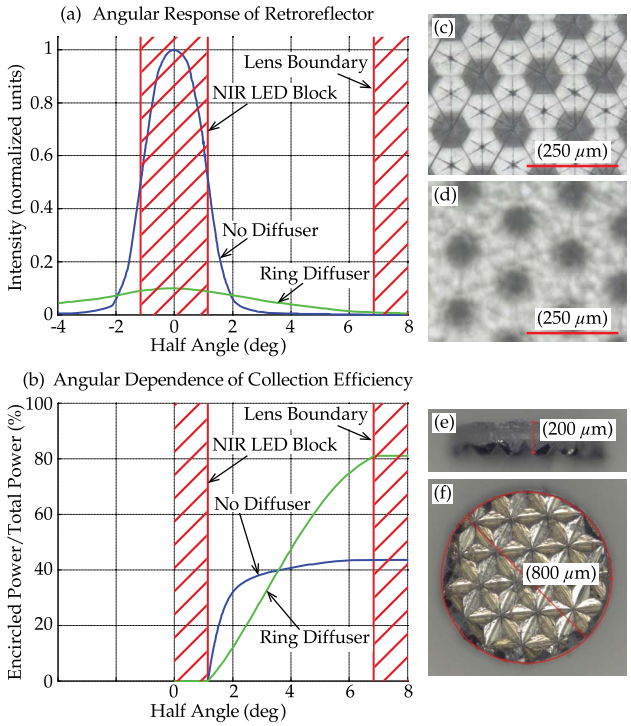

Fig. 5. (a) Angular dependence of retroreflected intensity. The cross-hatched area is either blocked by the NIR LED or lost outside the extent of the collection lens. (b) Ratio of encircled power to total power for each retroreflector configuration over the collection region. Note that the collected power ratio for the diffuser sample is twice that of the bare retroreflector when including the entire collection region. Photo showing (c) the front of a bare P66 retro and (d) the same retro modified with the imprinted ring diffuser as well as (e) the side view and (f) back view of a fully fabricated and punched diffusing retroreflector.

D. Polarizer Characterization

The extinction ratio of the stock PVA linear polarizer was measured before integration with a Melles Griot linear polarizer using a Keyence digital microscope to be 423:1 (99.8%). In an intact lens, the light transmitted through the annular polarizer is also sent through the four mirrors, which can introduce additional attenuation. To accurately measure the characteristics of the embedded polarizer alone, a fully integrated lens was sacrificed by grinding material from the back of the lens. This removed the first and third mirrors, as well as the back aperture, to leave intact the 1× and 2.8× apertures as well as the second and fourth mirrors. The polarizers remained embedded between the Paragon HI-154 polymer and PMMA layers, but can now be illuminated with polarized light from the rear (cut away) side of the lens to directly measure transmission. The two apertures are seen when mounted in front of a back-illuminated eye model and behind the Melles Griot linear polarizer (which is rotated to switch between apertures) in Fig. 7.

The extinction ratio of both embedded polarizers was measured [Fig. 8(c)] using the same microscope and analyzer to be 153:1 (99.3%). This contrast was achieved despite including areas with defects such as scratches, bubbles, and debris, as well as including the 11° clocking error which introduced some level

Fig. 6. Fabricated telescopic contact lens with embedded polarizers and diffusing retroreflector. The inset shows the retroreflector illuminated by a ring light around the camera and seemingly suspended fourth mirror.

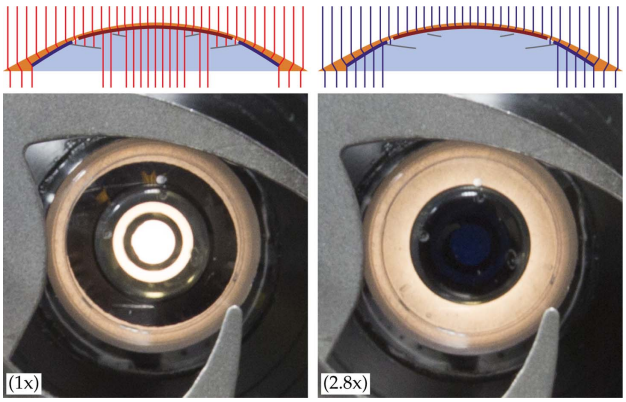

Fig. 7. Photos through the Melles Griot linear polarizer of the ground contact lens mounted in front of a back-illuminated eye model showing (left) 1× state (blocked 2.8× annular aperture) and (right) 2.8× state (blocked 1× circular aperture) with approximate optical paths shown in diagrams above.

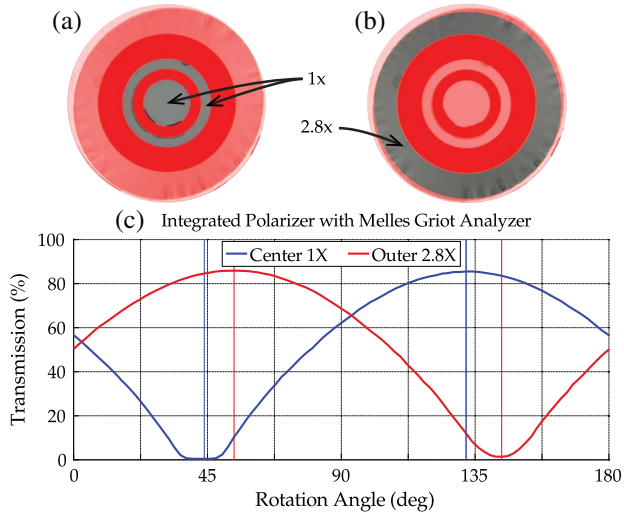

Fig. 8. (c) Angular dependence of embedded polarizer transmission with Melles Griot linear polarization analyzer where the colored vertical lines mark the extrema and their offset represents the clocking error. Images were collected with the entire area, then the intensity is integrated omitting the masked (red) regions for (a) the 1× and (b) the 2.8× path.

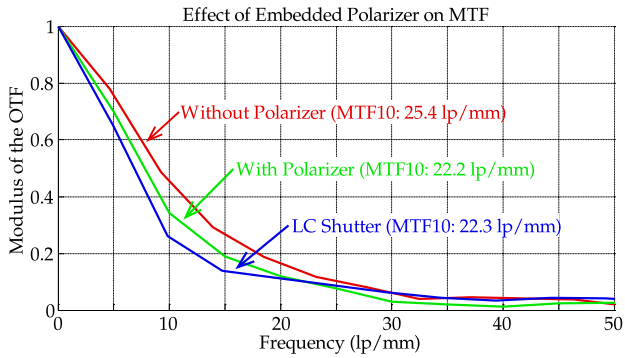

Fig. 9. MTF resolution measurements of fabricated contact lens with and without embedded polarizers (green and red), taken with a physical opaque block over the 1× aperture to avoid cross talk from the 1× optical path, and with the polarizer and LC shutter in the external switching eyewear (blue).

of cross talk between the two vision modes. The two apertures were differentiated by the digital masking shown in Figs. 8(a) and 8(b). In fact these measurements are limited by the dynamic range of the digital microscope, and so provide a lower bound on the actual extinction ratios.

To quantify the effect of the polarizers (including defects) on the performance of the lens, resolution measurements (Fig. 9) of the contact lenses with (green) and without (red) polarizers were obtained using an opaque 1× aperture block placed in contact with the center of the lens. Integrating the polarizers produced a 12.5% reduction in MTF10 (modulation transfer function) from 25.4 lp/mm to 22.2 lp/mm.

3. SWITCHING SYSTEM

The external switching system (Fig. 10) incorporates the lens assembly from a pair of Samsung SSG-4100GB 3D active glasses, modified by removing the rear linear polarization analyzer and which holds the NIR optics. The lenses are mounted on the frame from a pair of Revision "Sawfly" ballistic protection glasses, which also holds the switching control, and batteries. A NIR LED bonded to the center of a Fresnel collection lens above a IR detector is mounted to the bottom rim of each eyeglass lens. Temple-mounted electronics designed by Rockwell Collins include an AC-modulated LC shutter drive voltage and microcontroller which detects a wink due to the difference in reflectivity, and thus detected power, of the embedded retroreflector and eyelid by monitoring both eyes simultaneously. The electronics include a switch to toggle between continuous zoom and wink detection mode. The device is powered by two AAA batteries mounted on the opposite temple.

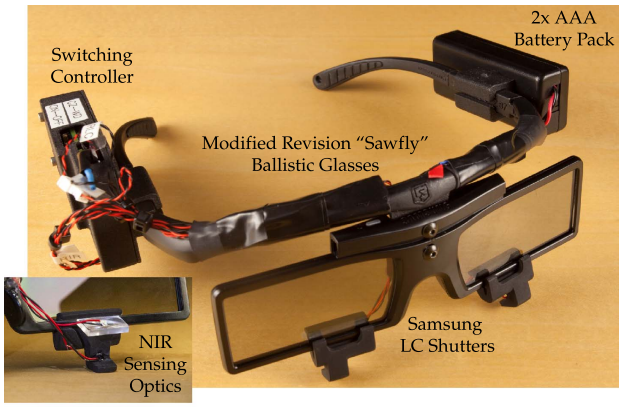

Fig. 10. Prototype switching glasses with self-contained temple-mounted wink/blink controller. The NIR sensing optics (LED, Fresnel lens, and detector) are mounted below the LC shutter windows to illuminate the contact lens, as shown in the inset.

A. Component Characterization

In the passive state, the switching system draws 55 mA at 3 V for a power consumption of 165 mW. After detecting a wink the Samsung LC shutters are driven by a ±10 V square wave modulated at 70 Hz, which switches to the active state, drawing 161 mA and increasing power consumption to 483 mW. The extinction ratio of the embedded polarizers and the LC shutters was measured using the same arrangement used in measuring Fig. 8(c), exchanging the static Melles Griot analyzer for the modified LC shutter to switch between passive and active states. The results are shown in Fig. 11. The extinction ratio of the passive LC shutter was 8:1 (87.3%) while the active LC shutter produced a ratio of 48:1 (97.9%), an asymmetry common to nematic LC modulators [12]. There was also some secondary wavelength dependence observed in the passive state due to the chromatic dispersion of the birefringent material [13,14].

The switching time of the LC shutter was measured by detecting the intensity of a laser passing though the shutter during turn-on (where the shutter is powered and switches from transparent to opaque) and turn-off (where the shutter is unpowered and switches from opaque to transparent).

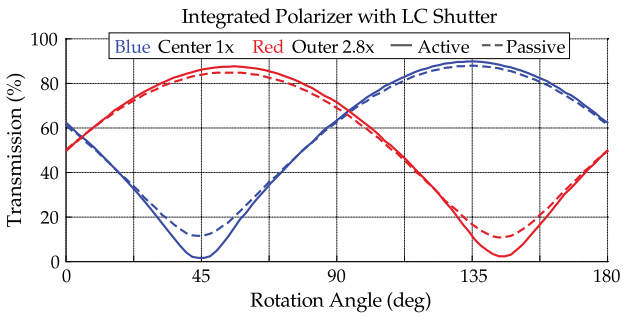

Fig. 11. Angular dependence of embedded polarizer transmission with Samsung LC shutter where the blue lines represent the center 1× path, the red lines represent the outer 2.8× path, the solid linestyle represents the LC active state, and the dashed linestyle represents the LC passive state.

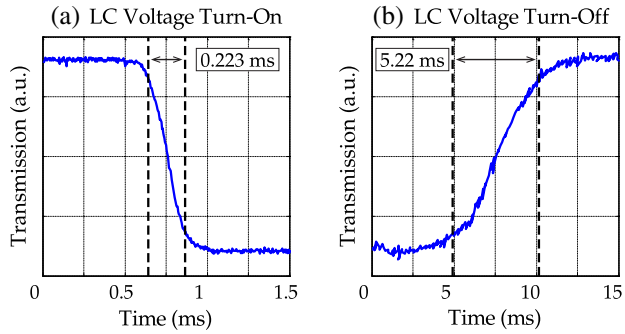

Fig. 12. Liquid crystal turn-on (a) and turn-off (b) transitions.

The LC voltage turn-on (90% to 10% transmission) and turn-off (10% to 90% transmission), indicated by dashed lines in Figs. 12(a) and 12(b), were 223 μs and 5.22 ms, respectively.

4. FULL SYSTEM TEST

Having characterized the individual components, the next step is to integrate and test the overall system and use the switching eyewear in conjunction with the fabricated contact lens. In the full system, the NIR LED illuminates a diffusing retroreflector embedded within the contact lens, which directs the return signal toward a Fresnel collection lens which focuses the light onto an IR detector (Fig. 10 inset). The eyewear can be set to manual operation, toggled by a small temple-mounted switch. When the system is set to wink-detection mode, the NIR LED light sources are turned on, and the detected signals from both eyes are monitored constantly by the electronics, which compares the two signals. Since blinking (simultaneous closure of both eyes between 100–400 ms [15]) is an involuntary action, blinks are detected and ignored by the electronics. Winking (closure of a single eye) is used to switch the state of the system, each eye controlling one vision mode.

The contact lens is aligned on the eye so the embedded polarizer over the 1× path is aligned to the passive state of the LC shutter, and the polarizer over the 2.8× path is perpendicular. This ensures that the 1× vision is the default mode (e.g., without electrical power). When a wink of the left eye is detected, the LC shutters are triggered and the polarization of the light entering the contact lens is switched. Now the light is blocked by the embedded polarizer over the 1× path but transmitted by the polarizer over the 2.8× path, switching to magnified vision. When a wink of the right eye is detected, the LC shutters are toggled off and revert to their inactive state and 1× vision.

For optical bench testing of the system, switching glasses are held in front of an imaging model eye with a 3D printed mount. A second nonimaging (dummy) eye "wearing" a contact lens is mounted with diffusing retroreflectors for the switching toggle. The full system used in testing is seen in Fig. 13. The contact lens is mounted on the eye model using distilled water orientated with the diffusing retroreflector positioned at the bottom and where the 2.8× polarizer is orthogonal to the passive polarization state of the LC shutter glasses. Capillary forces are sufficient to hold the lens stationary. Manually operated "eyelids" can move into place between the glasses and the contact lens, blocking the path between the NIR

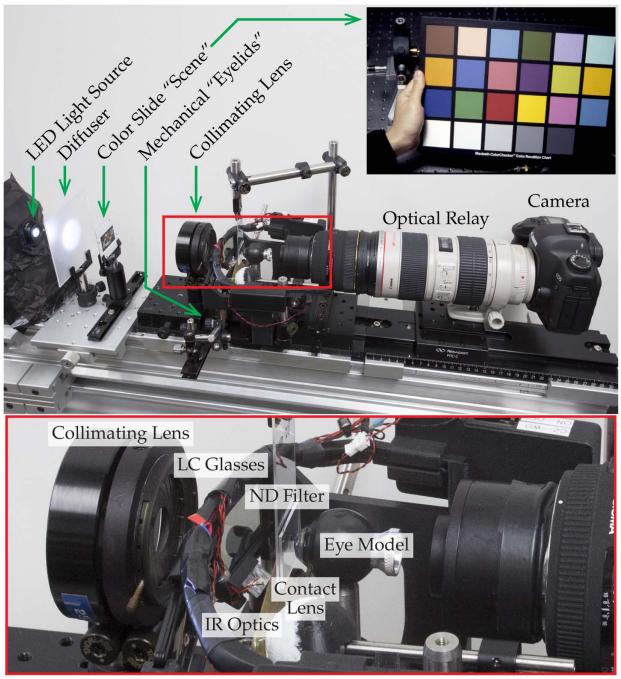

Fig. 13. Testing apparatus showing back-illuminated color slide "scene," collimating lens, switching glasses with IR optics, mechanical "eyelids," ND filter, contact lens mounted on eye model, optical relay, and camera.

LED and the embedded retroreflector. The eyelids are made of uncoated cardboard, which was found to have a similar reflectivity to skin.

The life-sized model eye [11] produces an image on the back of a fiber bundle which is passed through an optical relay made from a Sigma 50 mm F/1.4 DG HSM and a Cannon 70–200 mm F/2.8 IS USM lens with variable magnification to fill the sensor of a Cannon 5D Mark III SLR camera, allowing high-resolution still photographs and 1080p video operation. The resolution of the system is limited by the eye model optics, which matches the MTF of the Zemax human eye model. The imaged object was a back-illuminated color projection slide "scene" located at the focal plane of a 100 mm focal length lens, providing a brightly lit color scene at an apparent range of infinity.

Characterization of the optical performance of the two (unpolarized) vision paths can be found in [10]. In this earlier version of the lens, resolution of the 2.8× vision path was limited in resolution by the surface finish of the first (outer) surface, and by the internal mirror surface roughness. Surface characterization of the as-fabricated lens elements, including nonsequential modeling of the impact of surface roughness on the optical resolution of the 2.8× image, can also be found in [10].

For the current work, we refabricated the diamond turned optical inserts. This improved mirror roughness and adhesion, but unfortunately the enhanced aluminum mirrors had a thickness error that shifted the center wavelength and reduced reflectivity for the visible spectrum well below the >95% specification. Reflectivity measured from a single reflection ranged from 40%–50%. The overall magnified path transmission for 650 nm was approximately double that of 530 nm. With four internal reflections, the total transmission was measured to be 2%–6% over the visible spectrum, compared to the design goal of 82% and the 96% transmission of the refractive 1× path. Transmission is further reduced by 50% due to the polarizers.

Ideally, the inserts would have been fabricated again to enable lens prototypes with correct mirror surface, adhesion, and reflectivity. However, an additional fabrication was not practical with the available resources. To reduce the intensity cross talk and enable operation of the overall hands-free switching system, the brightness of the two paths were equalized by adding a circular neutral density (ND) filter with a 2.0 optical density in front of the 1× aperture.

Sample-dependent defocus between the two optical paths was observed in the fabricated lenses. This was traced to variation in the base radius of the aspheric front input surface. Determining the cause of this defect will require further fabrication iterations, but the source may be bowing of the 1.7 mm thick lens during mounting for the final process step, diamond turning of the outer surface. This was corrected by adding up to one diopter (depending on the specific lens) of power in front of the switching glasses. Since this correction has a much stronger effect on the magnified path than the unmagnified path due to the longer focal length, it was sufficient to axially move the collimating lens used to push the imaged object to infinity to bring the focal points closer together.

An example of the switched 1× and 2.8× output obtained with the full system is shown in Fig. 14. The contact lens was orientated to align the 2.8× polarizer with the active LC shutter

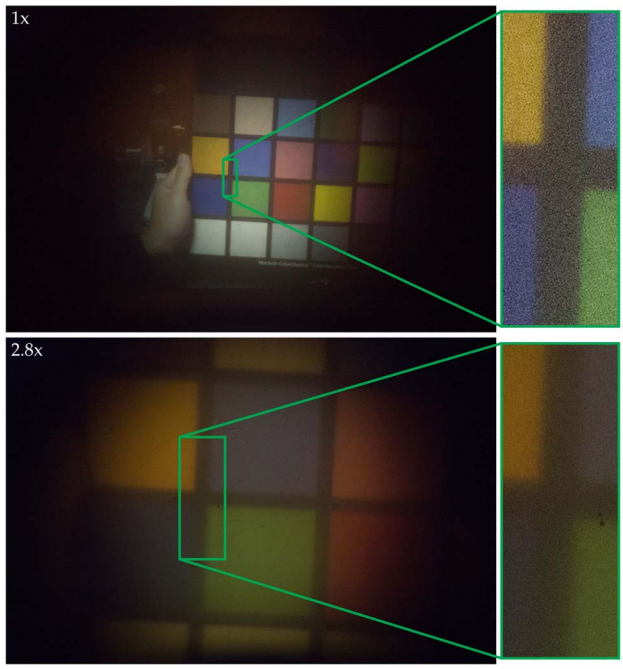

Fig. 14. Photos through 1× and 2.8× vision paths using the fully assembled contact lens and external LC glasses, captured with the testing apparatus at 1/30 s exposure and 12800 ISO. Magnification modes were selected using wink detection with the mechanical "eyelids."

state, as this yields the maximum extinction (Fig. 11). Some cross talk from the 2.8× image is transmitted into the 1× image (visible in the top photo in Fig. 14 as red shading just above the hand), which accounts for the reduction in contrast for low spatial frequencies in the resolution measurement of the lens with external switching glasses (see blue line in Fig. 9), and the spectral dependence of the reflectivity changes the 2.8× image white balance. To limit the switching cross talk to 5%, the embedded polarizers should be aligned to within 12.9° relative to each other, as compared to the 11° in the fully integrated lens sample tested. To achieve a switching cross talk of 1%, small compared to the maximum 48:1 active LC shutter contrast, they should be aligned to within 5.7° rotational error. This accuracy was achieved in some of the nonoptical samples, and should become repeatable with some process development. Detailed characterization of the optical resolution and the reasons behind the degradation of the 2.8× image can be found in [10].

The integrated system was successfully operated, using the manual blink and wink "eyelid" shutters, and provided reliable switching between the 1× and 2.8× vision states, given a relatively long (~0.5second) wink of the right and left eye, respectively. Rapid winks and blinks were ignored. The response of the switching system was measured when switching from 1× to 2.8× [Fig. 15(a)] and from 2.8× back to 1× [Fig. 15(b)] using the same system as used in Fig. 12 by blocking the retroreflected NIR beam path for sufficient time to trigger a wink detection. The systems exclusion of blinking is shown in Fig. 15(c).

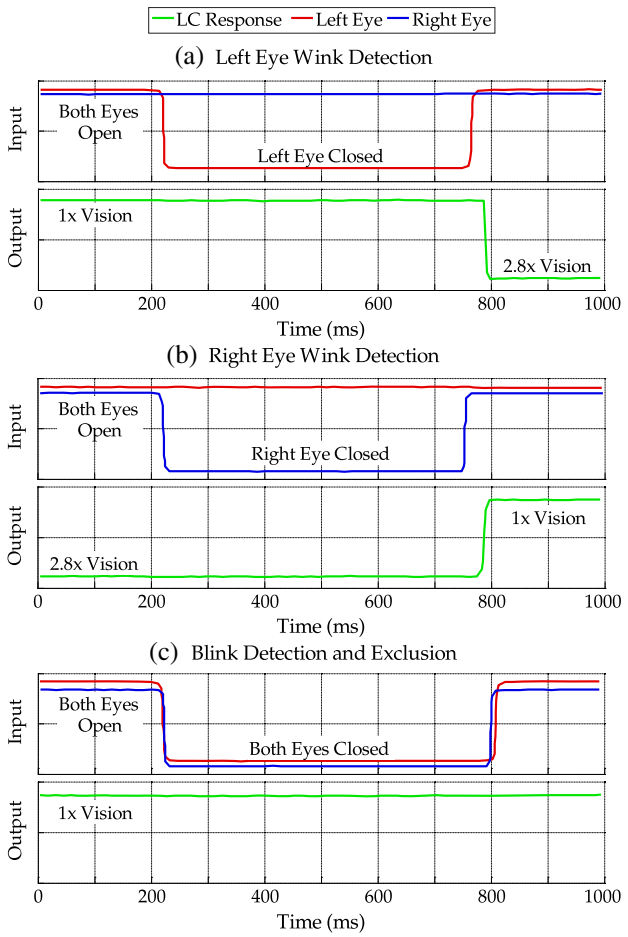

Fig. 15. Response of switching glasses when detecting (a) left eye wink and switch to 2.8× vision, (b) right eye wink and switch back to 1× vision, and (c) blink detection and exclusion thereby remaining in 1× vision.

5. SUMMARY AND CONCLUSIONS

We have fabricated telescopic contact lenses with embedded linear polarizers that differentiate between the 1× and 2.8× optical paths, as well as diffusing retroreflectors to aid in switching. We fabricated fully self-contained eyewear, including polarization shutters, control electronics and battery power, and wink-operated switching. We operated the system on the optical bench using a scale model human eye and mechanical "eyelids," establishing feasibility of an active vision augmentation system with hands-free zoom and switching.

This technology requires further refinement for practical application. The contact lenses' fabrication tolerances need to be improved to reach the design resolution. The mirrors must provide at least 95% reflectivity to produce bright images for both magnifications, and the diamond turning of the front surface, specifically in the annular 2.8× aperture, should be improved to eliminate the sample-dependent defocus. The lens also needs structural modification to allow extended wear. One path to this goal, scleral contact lenses that incorporate an internal air cavity to allow oxygen flow around a gas impermeable telescope insert, is a subject of on-going development.

Funding. Defense Advanced Research Projects Agency (DARPA) (W911NF-11-C-0210).

Acknowledgment. The authors thank William Meyers and Kirk Reed at Paragon Vision Sciences for their expertise in scleral contact lens design and fabrication, and William M. Mellette and other members of the UCSD Photonic Systems Laboratory for helpful technical discussions.

REFERENCES

1. E. Peli, "The optical functional advantages of an intraocular low-vision telescope," Optom. Vis. Sci. **79**, 225–233 (2002).
2. S. S. Lane and B. D. Kuppermann, "The implantable miniature telescope for macular degeneration," Curr. Opin. Ophthalmol. **17**, 94–98 (2006).
3. N. Orzalesi, C. O. Pierrottet, S. Zenoni, and C. Savaresi, "The iol-vip system: a double intraocular lens implant for visual rehabilitation of patients with macular disease," Ophthalmology **114**, 860–865 (2007).
4. L. Amselem, M. Diaz-Llopis, A. Felipe, J. M. Artigas, A. Navea, and S. García-Delpech, "Clinical magnification and residual refraction after implantation of a double intraocular lens system in patients with macular degeneration," J. Cataract Refract. Surg. **34**, 1571–1577 (2008).
5. J. Tabernero, M. A. Qureshi, S. J. Robbie, and P. Artal, "An aspheric intraocular telescope for age-related macular degeneration patients," Biomed. Opt. Express **6**, 1010–1020 (2015).
6. A. Agarwal, I. Lipshitz, S. Jacob, M. Lamba, R. Tiwari, D. A. Kumar, and A. Agarwal, "Mirror telescopic intraocular lens for age-related macular degeneration: design and preliminary clinical results of the lipshitz macular implant," J. Cataract Refract. Surg. **34**, 87–94 (2008).
7. A. Isen, "Feinbloom miniscope contact lens," Encycl Contact Lens Pract. **13**, 53–55 (1963).

8. E. J. Tremblay, R. A. Stack, R. L. Morrison, and J. E. Ford, "Ultrathin cameras using annular folded optics," Appl. Opt. **46**, 463–471 (2007).
9. E. J. Tremblay, I. Stamenov, R. D. Beer, A. Arianpour, and J. E. Ford, "Switchable telescopic contact lens," Opt. Express **21**, 15980–15986 (2013).
10. A. Arianpour, G. M. Schuster, E. J. Tremblay, I. Stamenov, A. Groisman, J. Legerton, W. Meyers, G. A. Amigo, and J. E. Ford, "Wearable telescopic contact lens," Appl. Opt. **54**, 7195–7204 (2015).
11. A. Arianpour, E. J. Tremblay, I. Stamenov, J. E. Ford, D. J. Schanzlin, and Y. Lo, "An optomechanical model eye for ophthalmological refractive studies," J. Refract. Surg. **29**, 126–132 (2013).
12. V. N. H. Silva, "Liquid crystal shutters for stereoscopic vision and 3d dual view application," Ph.D. thesis (Télécom Bretagne, Université de Bretagne-Sud, 2013).
13. C. Gooch and H. Tarry, "The optical properties of twisted nematic liquid crystal structures with twist angles $\leq$ 90 degrees," J. Phys. D **8**, 1575–1584 (1975).
14. A. K. Srivastava, J. de Bougrenet de la Tocnaye, and L. Dupont, "Liquid crystal active glasses for 3d cinema," J. Disp. Technol. **6**, 522–530 (2010).
15. R. Milo, P. Jorgensen, U. Moran, G. Weber, and M. Springer, "Bionumbers–the database of key numbers in molecular and cell biology," Nucleic Acids Res. **38**, D750–D753 (2010).